Int J Adv Manuf Technol (2015) 81:1863–1870
DOI 10.1007/s00170-015-7224-x

ORIGINAL ARTICLE

Comparison of two setups for induction heating in injection molding

Stefano Menotti[1] · **Hans Nørgaard Hansen**[1] · **Giuliano Bissacco**[1] · **Patrick Guerrier**[1] · **Peter Torben Tang**[2]

Received: 23 January 2015 / Accepted: 26 April 2015 / Published online: 30 May 2015

Abstract To eliminate defects and improve the quality of molded parts, increasing the mold temperature is one of the applicable solutions. A high mold temperature can increase the path flow of the polymer inside the cavity allowing reduction of the number of injection points, reduction of part thickness, and moulding of smaller and more complex geometries. The last two aspects are very important in micro injection molding. In this paper, a new embedded induction heating system is proposed and validated and two different coil setups were tested and compared. An experimental investigation was performed based on a test geometry integrating different aspect ratios of small structures. Acrylonitrile butadiene styrene (ABS) was used as material, and different mold temperatures were tested. The replicated test objects were measured by means of an optical coordinate measuring machine (CMM). On the basis of the experimental investigation, the efficacy of the two induction embedded coils, with respect to improvement of replication quality, has been verified.

Keywords Micro injection molding · Tooling · Induction heating system · Optical CMM

1 Introduction

In recent years, the requirements on geometrical accuracy of plastic products have increased while products got smaller and thinner [1]. Not always conventional, injection molding could satisfy the requirements. For that reason, different companies have developed and introduced heating systems to increase the mold temperature to obtain a better quality of the molded objects. The most common heating technologies used nowadays are resistive heating, hot fluid/steam in the cooling channels, infrared lamp heating, laser light, and external induction heating [2–5]. At the same time, an increase of the mold temperature has the drawback to prolong the total cycle time for the single molding.

A new embedded induction system was designed and investigated with focus on improvement of replication quality while maintaining short total cycle time. For the validation of the system, an experimental investigation was performed based on a test geometry integrating different aspect ratios of small structures in ABS.

In this study, two different coil setups were investigated: the first one consists in a massive coil "bulk coil" while the second one was a small flat one "pancake coil."

The performances of the two setups were evaluated considering the replication quality obtained by the overall injection molding cycle.

2 Induction heating system

In the fixed mold part, an electrical induction coil is installed to heat the surface of a small defined area of the cavity, and on the movable side, conventional cooling channels are set.

The induction heating system is mainly consisting of a power supply to increase the frequency of the AC from 50 up to 10 KHz, a transformer, a capacitor, and an induction coil to be positioned inside the base mold just behind the test geometry (Fig. 1) [6].

✉ Stefano Menotti
steme@mek.dtu.dk

[1] Department of Mechanical Engineering (MEK), Technical University of Denmark (DTU), DK – 2800 Kgs. Lyngby, Denmark

[2] IPU, 2800 Kgs. Lyngby, Denmark

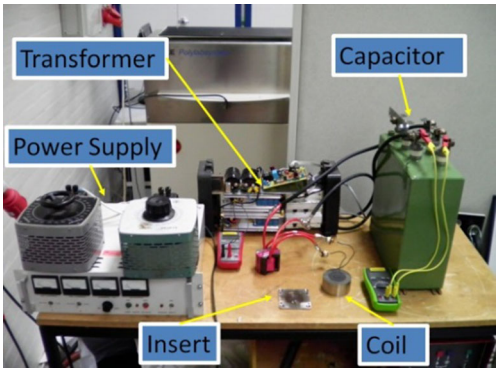

Fig. 1 Layout of the induction system [6]

This new induction heating experimental setup has the characteristic of working in a completely automatic manner to ensure a high repeatability of the process conditions. The main steps of the process are the following. First, the injection machine closes the two parts of the mold, and at the same time, it sends an electrical signal to the induction system that activates the heating time. When the predetermined time is over, the machine injects the polymer in the cavity. At this point, the cooling time starts, and when the ejection temperature is reached, the test part is ejected. After that the cycle starts over again. The adjustable parameters on the external induction system are the heating time and the input power. The power can vary changing the voltage on the power supply. In the following experiments, the input power was fixed at 3335 W.

2.1 Setup of the first coil: bulk coil

The first induction coil assembly, named bulk coil, is made of a hollow copper-insulated tube for the circulation of cooling water. The coil is inserted in a ferrite core to concentrate the magnetic field in a specific area. The connection between the coil and the ferrite core is provided by a thermally conductive concrete powder (Fig. 2). The ferrite core and the coil are inserted in a metallic cylinder to give it a higher mechanical strength. In Fig. 3, a cross-sectional view of the coil is reported. The overall dimensions of the metallic cylinder are 80 mm in diameter and 40 mm in height. On the top of the coil, a K type thermocouple is mounted to measure the temperature in the center of the setup.

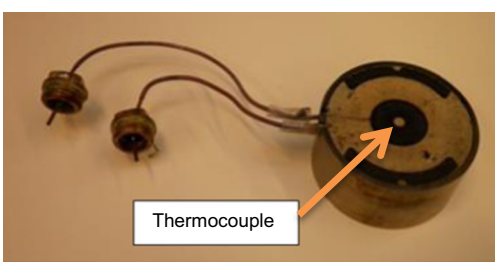

Fig. 2 First coil, bulk coil

2.2 Setup of the second coil: pancake coil

The second induction coil assembly, named pancake coil, is made of a copper litz wire (Fig. 4) insulated with a high heat resistance shrinkage tube. The litz wire coil has the characteristic to reduce the skin effect and proximity effect losses at medium and high frequency [7]. The litz wire is inserted in a milled spiral grove in a Somaloy substrate. This material which consists of a compound of iron powder in a polymer binder is chosen to reduce losses compared to an iron powder core [8]. Also in this setup, the Somaloy material is used to concentrate the magnetic field in a specific area. The pancake coil has a thickness of only 5 mm and an outside diameter of 40 mm. In this case, for preventing an over-heating of the wire, a dedicated cooling system was positioned underneath. Similarly to the previous one also in this setup, on the top of the coil, a K type thermocouple was mounted to measure the temperature in the center of the setup (Fig. 5).

In Fig. 6, examples of the cavity mold temperature profile during the injection process are shown. In the figure, four different plots with different heating times are shown. In each of the four graphs, the temperature profiles of the two different coils for the same process parameters are reported. The moldings were done with a constant injection velocity of 20 mm/s and a cooling temperature of 20–25 °C. The cooling time was varied together with the heating time between the two coils to compensate for the different mold cavity temperatures reached. It is possible to notice that an increase of the heating time of 2 s corresponds to an increase of the mold temperature of approximately 20 °C, meaning a heating ratio of 10 °C/s. In literature, other researchers obtained a temperature gradient of 4 °C/s with a similar setup [9]. The cooling time in this specific series of experiments was increased from 0 to 15 s when the heating time was set at 4 s to reach the ideal demolding temperature. An adjustment of the cooling time was necessary just for the bulk coil. From the temperature graph, it is possible to appreciate the different behavior of the two coils. The pancake coil shows a higher heating rate and a higher max temperature compared to the bulk one. The same trend, higher cooling rate associate with a lower temperature is shown in the cooling phase due to more effective cooling system positioned just behind the coil.

3 Test geometry

The selected feature for these experiments is a simple comb with four cantilevers of 15-mm length and 3-mm width. The

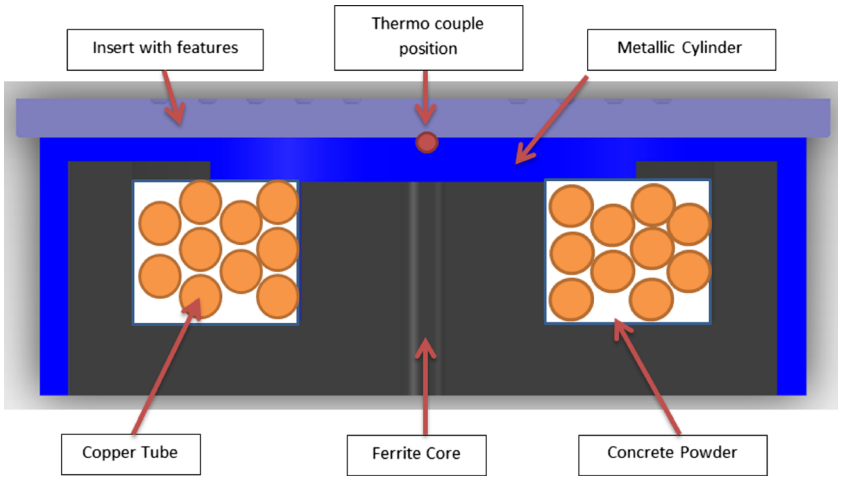

Fig. 3 Schematic view of the bulk coil

four cantilevers have different thicknesses, 0.1, 0.3, 0.5, and 0.7 mm, respectively (Fig. 7). The test geometry was designed to give a quick characterization of the polymer melt behavior in the cavity and also to allow a relatively simple measurement procedure.

The main body of the cavity just before the four cantilevers has a cavity depth of 1.5 mm where the material could be expanded and homogenized before entering into the cantilevers. Four venting channels were manufactured at each cantilever end to improve air evacuation. A milling process was used to generate the cavities. The outside dimension of the insert is 85 mm×85 mm×4 mm, and the material is a pre-hardened tool steel (IMPAX). Figure 8 shows the manufactured insert.

In Fig. 9, a representation of the test part is reported.

4 Experimental micro injection molding

The experimental plan for the validation of the two developed induction coils and induction heating systems is reported in Tables 1 and 2. The process parameters varied in the experimental plan were the heating time and the type of induction coil.

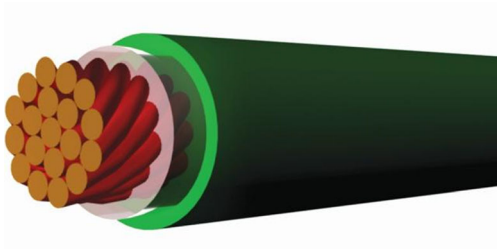

Fig. 4 Schematic view of a litz wire

The injection velocity was fixed at a low value of 20 mm/s. The max pressure value was fluctuating around an average value of 530 bar. The packing pressure was set as half of the injection pressure value 265 bar.

Different combinations of heating time and cooling time were tested. The experiments were carried out with the base mold temperature at the lowest temperature reachable from the system of approximately 22 °C.

The induction heating time was increased from 0 s up to a max value of 6 s with steps of 2 s.

The molding experiments were carried out on an Arburg Allrounder 370A 600-70 all drive injection machine with a diameter of the screw of 18 mm.

In all the experiments, the packing time was set constant at the value of 6 s. The material used in the experiments was ABS (Acrylonitrile Butadiene Styrene) with the properties shown in Table 3.

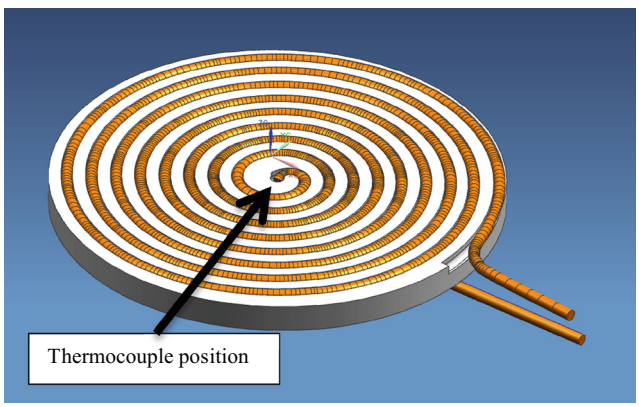

Fig. 5 Second coil, pancake coil

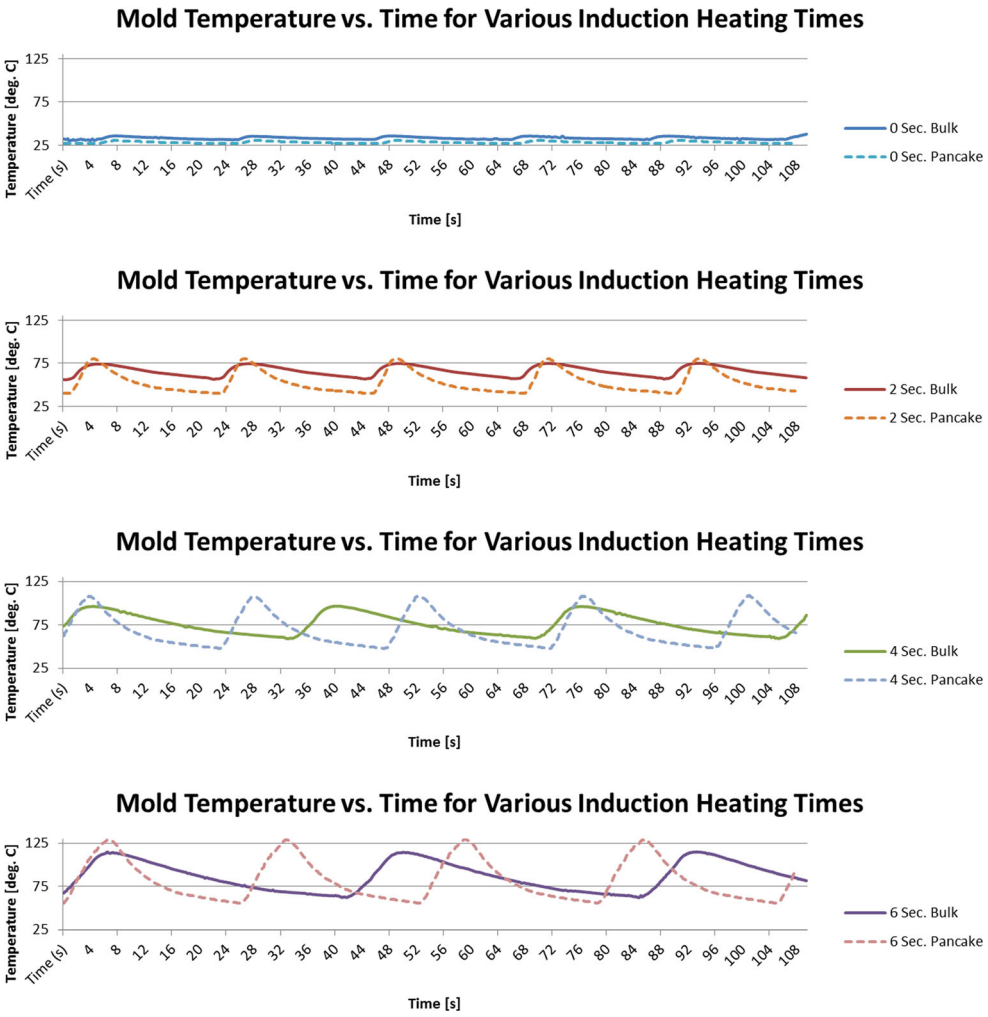

Fig. 6 Example of cavity mold temperature during the process at different heating times

5 Measurement strategy

To compare the effect of different process settings on the filling of the part, the length of each sample's cantilever was measured. An optical measurement device, DeMeet 220 by Schut Geometrical Metrology, was used to perform these measurements. A combination of user inputs and program-defined measurements was used to perform length measurements.

Prior to the measurements, each sample was labeled and the runner system was removed. The samples were then attached to a fixture using double tape for consistent placement on the device platform (Fig. 10).

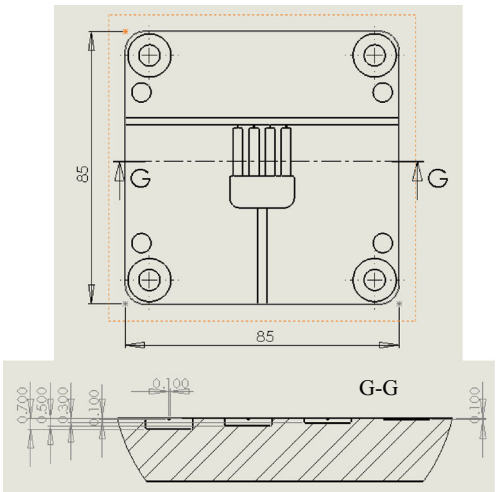

Fig. 7 Front and cross section views of the insert [6]

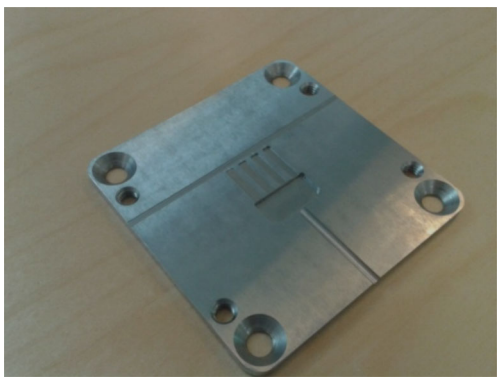

Fig. 8 Mold insert [6]

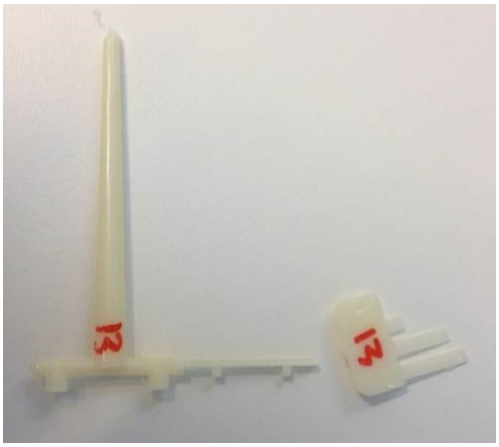

Fig. 9 Example of molded part [6]

Before running the program to collect length measurements, references were defined for each cantilever. The camera of the device was focused on the top surface of each cantilever. The measurement locations remained consistent across the width of the cantilevers, while the Z focal position was adjusted to find the ending edge along the length.

The program searched for two points at the end of each cantilever. The user verified that these points were at the edge of each cantilever. The program was run for each of the 20 samples collected for each experiment. Adjustments were made to measurement planes and locations when the program failed to locate a point along the cantilever's end or when the program located a point incorrectly.

6 Uncertainty analysis on the optical measurement

An uncertainty analysis was completed in order to assess the accuracy of the cantilever length measurements. One sample was measured 20 times to determine the repeatability of the measurements. The sample was fully removed from the fixture and platform and then replaced. Another source of uncertainty considered in this analysis was from the measuring instrument. The maximum permissible error of the machine was used as the measuring instrument uncertainty. Using the polymer part thermal expansion coefficient, the bias in length from the environmental temperature was removed [10].

Table 1 Process settings (bulk coil)

Ex	Velocity (mm/s)	Cooling T (°C)	Cooling Time (s)	Heating Time (s)
1	20	20–25	*0*	**0**
2	20	20–25	*0*	**2**
3	20	20–25	*15*	**4**
4	20	20–25	*20*	**6**

Table 2 Process settings (pancake coil)

Ex	Velocity (mm/s)	Cooling T (°C)	Cooling Time (s)	Heating Time (s)
1	20	20–25	*0*	**0**
2	20	20–25	*0*	**2**
3	20	20–25	*0*	**4**
4	20	20–25	*0*	**6**

An example calculation is shown below.
Average of 20 measurements:

$$\overline{L} = \text{Average of } L$$

Thermal expansion coefficient:

$$\text{TCE} = 0.090\ [\text{mm/m}{-}℃] \text{ at } 20.0℃$$

u_p standard uncertainty from procedure (repeatability of measurements):

$$u_p = \text{std. dev. of 20 samples}$$

u_m standard uncertainty from measuring instrument:

$$u_m = \text{MPE} = 0.005 \text{ mm}$$

u_e standard uncertainty from environment (temperature):

$$u_e = (T{-}T_{ref})(\text{TEC})(\overline{L})(b) = 0.001 \text{ mm}$$

$$T = \text{Room temperature } 21\ ^\circ\text{C}$$

$$b = 0.7\ (U \text{ distribution is assumed})$$

Combined standard uncertainty:

$$u_c = \sqrt{{u_m}^2 + {u_e}^2 + {u_p}^2}$$

Result (with coverage factor, k=2):

$$L = \overline{L} \pm k \times u_c\ mm = \overline{L} \pm U$$

The calculated expanded uncertainty with a confidence level of 95 % is reported in Table 4.

Table 3 Material properties as indicated in the material data sheet

Property	Value
Commercial name	Novodur P2H-AT
Producer	Styrolution
Density	1.05 g/mm^3
Drying temperature	80 °C
Drying time	2 to 4 h
Processing temperature	220 to 260 °C

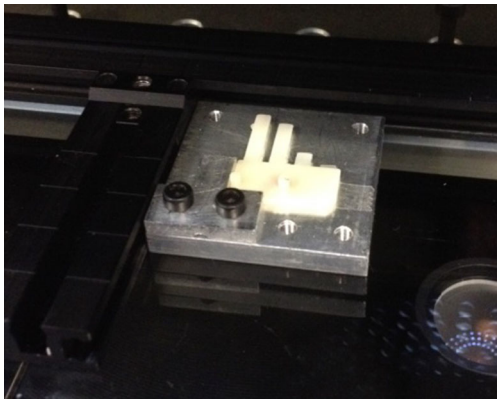

Fig. 10 Position of the test geometry on the optical CMM

Table 4 Uncertainties for the four fingers

	Finger thickness (mm)			
	0.7	0.5	0.3	0.1
Average of L	14.928	11.875	3.739	0.656
u_p	0.001	0.008	0.010	0.032
u_m	0.005	0.005	0.005	0.005
u_e	0.001	0.001	0.000	0.000
u_c	0.005	0.009	0.011	0.032
U	0.010	0.018	0.022	0.064

From Table 4, it is possible to notice that the total uncertainty U is in the same magnitude order for the four finger thickness.

7 Results and discussion

Fig. 11 reports the measured lengths of the four cantilevers at different processing conditions and type of coil.

From the graph, it is possible to observe that an increasing of heating time and consequently an increasing of the mold temperature promote a better replicability of the cavity geometries. In fact, the polymer cantilevers are getting longer and longer in correlation with the increase of temperature. It is possible to observe this aspect in both the two considered setups for the induction coil.

If we make a consideration regarding the performance of the two coils, it is possible to appreciate that with the bulk coil, it is possible to obtain a longer polymer path inside the cavity.

In Table 5, a comparison between the flow length obtained with the bulk coil and the pancake coil is reported in terms of deviation between the two different setups.

The Dev% was defined as follows:

$$\mathrm{Dev}\% = \frac{\mathrm{Lenght}_{\mathrm{bulk}} - \mathrm{Lenght}_{\mathrm{pancake}}}{\mathrm{Lenght}_{\mathrm{pancake}}} \times 100$$

where $\mathrm{Lenght}_{\mathrm{bulk}}$ refers to the length of the single cantilever obtained with the bulk coil and $\mathrm{Lenght}_{\mathrm{pancake}}$ refers to the length of the single cantilever obtained with the pancake coil.

Table 5 clearly shows that with the bulk coil, it is possible to obtain a longer flow path of the polymer inside the cavity; if we consider the cantilever with thickness 0.3 mm in the third and fourth experiments, the length is circa 70 % more longer than the one obtained with pancake coil.

This result could sound quite strange if we correlate it with the temperature measure from the thermocouple (Fig. 6). In fact, the temperature graphs show that the higher temperatures at the same molding temperature were reached with the pancake coil setup. From previous study [6, 11] with the bulk coil, we know that the better replication should be obtained with the highest temperature.

To explain this behavior, the position of the heat generation inside the insert and where the insert temperature is measured should be taken into consideration.

In fact, with the bulk coil, we have a high heat generation in a volume positioned above the ferrite core; whereas in the pancake coil, the heat generation is more uniform through the volume of the insert.

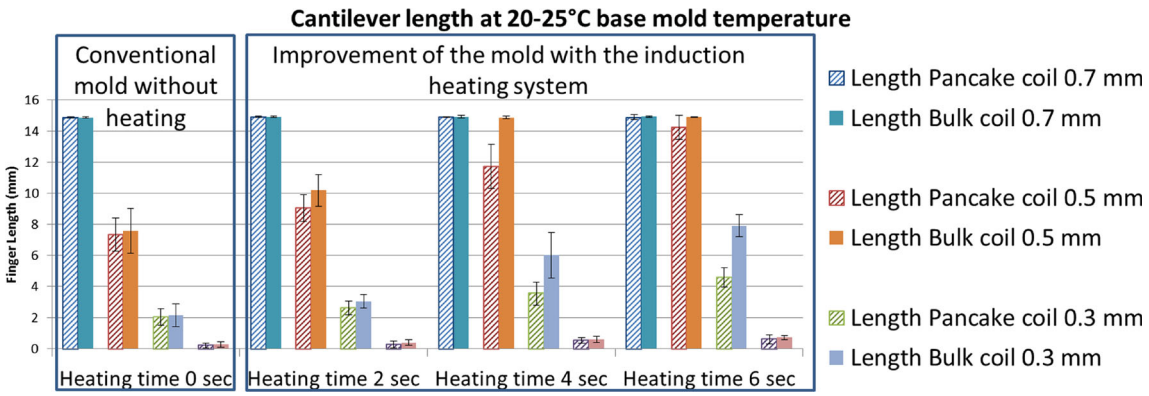

Fig. 11 Cantilever length value reached by the polymer at 20–25 °C base mold temperature

Table 5 Deviation of the flow length between the two coil setups

Cantilever	Experiment number			
Thickness	1	2	3	4
0.7	−0.08	−0.01	0.06	0.19
0.5	3.32	12.47	26.67	4.67
0.3	4.88	15.99	69.46	72.45
0.1	33.66	47.13	10.23	17.32

This behavior is possible to notice in the following two simulations where the two models of the coil were reproduced.

The simulation model for the pancake coil is axisymmetric which is represented by half of the coil. The entire system is modelled with four sections of the geometries that represent the different materials present in the coil setup. The litz wires are simplified by circles in eight square cavities, immersed in the Somaloy material. In each spiral, a current of 50.6 A and a frequency of 11.23 kHz were set. The cooling channel is modelled as a circle with a constant boundary temperature of 25 °C.

Also, the model of the bulk coil is axisymmetric. The entire system is modelled with seven overall sections which correspond to the different materials present in the coil setup. The hollow copper wires are modelled inside the cement and surrounded by the ferrite material. In each spiral, a current of 52.4 A and a frequency of 11.7 kHz were set. The cooling channels inside each of the hollow copper tubes were modelled using a constant temperature of 25 °C.

From the simulation result seen in Figs. 12 and 13, it is possible to observe and compare the temperature inside the insert and on the surface of the two setups. In the pancake coil, like mentioned before, the generation of heat is much more homogenous compared to the bulk coil, where the heat is mainly generated in a concentrated area. In the pancake coil and in the bulk coil, the thermocouple sensors were positioned in the points marked with (1). (2) is referring to the temperature of the gate. With the explanation of the position of the thermocouple sensor, it is possible to understand that in the pancake coil setup, the temperature measured was the maximum temperature of the insert; in the bulk coil, it was not the maximum temperature but we have an idea of the maximum temperature from the simulation. The dimensional scales of the two simulations are different due the different dimensions of the two coils as mentioned before.

For a more detailed explanation of the simulation setup, please refer to [12].

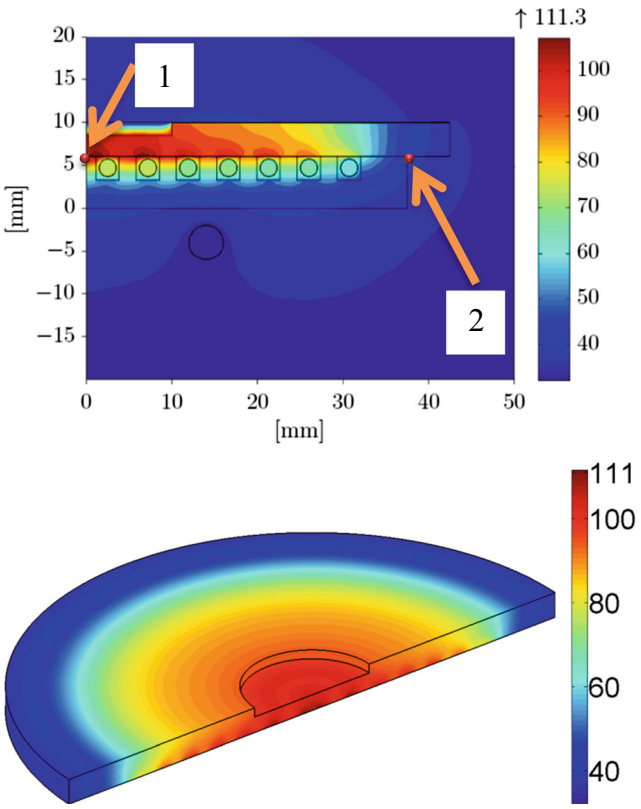

Fig. 12 Model of the pancake coil. *1* indicates thermocouple sensors. *2* indicates the temperature of the gate

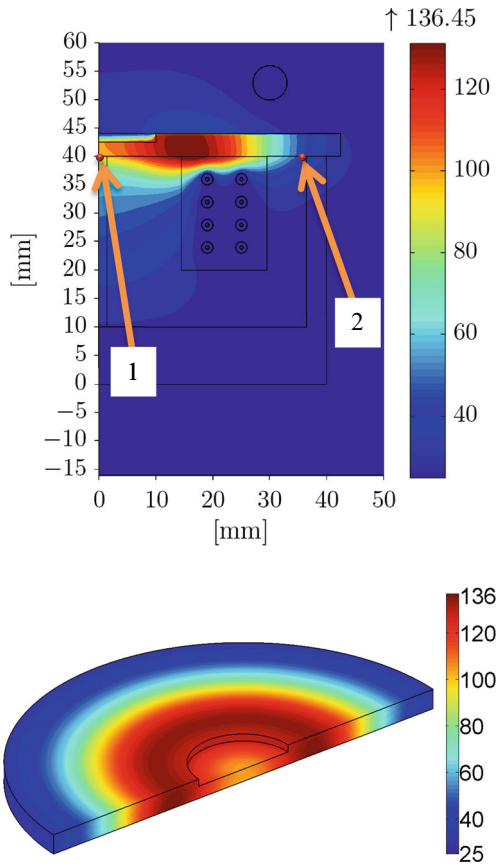

Fig. 13 Model of the bulk coil. *1* indicates thermocouple sensors. *2* indicates the temperature of the gate

With this observation, it is possible to understand why the coil with the highest measured temperature is not the most efficient in terms of replication quality. With this work, we understood that the pancake setup is not the best solution regarding the polymer (flow) replication but we are sure it is the right choice for other studies such as shrinkage and warpage for the homogeneity of the surface temperature.

8 Conclusions

This study investigates the effects of rapid mold-surface induction heating on the replication ability of a test geometry with thin and long features in ABS. In this work, two different induction coils were used and compared. The first coil was a very massive one (bulk) and the second a flat one (pancake).

An experimental plan, varying heating/cooling parameters, was carried out. The evaluations of the injection molding capability in replicating the micro test part were assessed through coordinate measuring machine (CMM) measurements of the lengths of four different long features.

The results show a clear trend regarding the improvement of the replica quality adding an external heating source during the molding.

Results showed better replication fidelity for the bulk coil system compared with the pancake coil system, but at the same time, the heat generation of the pancake coil is more uniform on the mold surface.

Acknowledgments The present research was carried out within the Innomold project (Innovative Plastic Products and More Energy Efficient Injection Molding Processes) supported by the Danish Council for Technology and Innovation.

References

1. Berger GR (2014) Influence of mold surface temperature on polymer part warpage in rapid heat cycle molding. AIP Conf Proc 1593: 189–194
2. Michaeli W, Schöngart M, Klaiber F, Beckemper S (2011) Variothermal injection moulding of superhydrophobic surfaces, in 7th International Conference on Multi-Material Micro Manufacture, pp 978–981
3. Chen S, Engineering M, Yuan C (2009) Rapid thermal cycling of injection molds: an overview on technical approaches and applications. Adv Polym Technol 27(4):233–255
4. Menotti S (2013) Initial verification of an induction heating set-up for injection molding. ANTEC 2013 Conf. Proc., pp 1485–1489
5. County H (2011) The effects of various variotherm processes and their mechanisms on injection molding. Intern Polym Process, 265–274
6. Menotti S (2014) Micro injection molding of thin walled geometries with induction heating system. Proc ICOMM
7. Litz wires [Online]. Available: http://www.newenglandwire.com/products/litz-and-formed-cables/types-and-constructions.aspx. [Accessed: 23-Sep-2014]
8. Somaloy [Online]. Available: http://www.hoganas.com/Documents/Segmentbrochures/Somaloy/Somaloy_Technology_October_2013_0600HOG.pdf. [Accessed: 23-Sep-2014]
9. Sung Y, Hwang S (1848) Design of an insert type induction heating and cooling system for injection moulding processes. Teh vjensnik 3651:651–656
10. Chiffre L D (2010) Geometrical metrology and machine testing: compendium, course 41731, January 2010. DTU
11. Menotti S, Hansen H N, Bissacco G, Calaon M, Tang P T, Ravn C (2014) Injection molding of nanopatterned surfaces in the submicrometer range with induction heating aid. Int J Adv Manuf Technol
12. Guerrier P, Nielsen KK, Hattel JH, Menotti S (2015) An axisymmetrical non-linear finite element model for induction heating in injection molding tools, ongoing research